ISSN 0016-7037
Volume 75, Number 1
January 1, 2011

Geochimica et Cosmochimica Acta

JOURNAL OF THE GEOCHEMICAL SOCIETY
AND THE METEORITICAL SOCIETY

Volume 75, Number 1 January 1, 2011

Articles

Continued on outside back cover

(This is a sample cover image for this issue. The actual cover is not yet available at this time.)

Available online at www.sciencedirect.com

SciVerse ScienceDirect

Geochimica et Cosmochimica Acta 75 (2011) 6584–6599

Geochimica et Cosmochimica Acta

www.elsevier.com/locate/gca

Kinetics of neptunium(V) sorption and desorption on goethite: An experimental and modeling study

Ruth M. Tinnacher [a,*], Mavrik Zavarin [a], Brian A. Powell [b], Annie B. Kersting [a]

[a] *Glenn T. Seaborg Institute, Physical and Life Sciences Directorate, Lawrence Livermore National Laboratory, P.O. Box 808, Livermore, CA 94550, USA*

[b] *Dept. of Environ. Eng. and Earth Sciences, Clemson University, Clemson, SC 29625, USA*

Received 19 November 2010; accepted in revised form 9 August 2011

Abstract

Various sorption phenomena, such as aging, hysteresis and irreversible sorption, can cause differences between contaminant (ad)sorption and desorption behavior and lead to apparent sorption 'asymmetry'. We evaluate the relevance of these characteristics for neptunium(V) (Np(V)) sorption/desorption on goethite using a 34-day flow-cell experiment and kinetic modeling. Based on experimental results, the Np(V) desorption rate is much slower than the (ad)sorption rate, and appears to decrease over the course of the experiment. The best model fit with a minimum number of fitting parameters was achieved with a multi-reaction model including (1) an equilibrium Freundlich site (site 1), (2) a kinetically-controlled, consecutive, first-order site (site 2), and (3) a parameter $\psi_{2,de}$, which characterizes the desorption rate on site 2 based on a concept related to transition state theory (TST). This approach allows us to link differences in adsorption and desorption kinetics to changes in overall reaction pathways, without assuming different adsorption and desorption affinities (hysteresis) or irreversible sorption behavior a priori. Using modeling as a heuristic tool, we determined that aging processes are relevant. However, hysteresis and irreversible sorption behavior can be neglected within the time-frame (desorption over 32 days) and chemical solution conditions evaluated in the flow-cell experiment. In this system, desorption reactions are very slow, but they are not irreversible. Hence, our data do not justify an assumption of irreversible Np(V) sorption to goethite in transport models, which effectively limits the relevance of colloid-facilitated Np(V) transport to near-field environments. However, slow Np(V) desorption behavior may also lead to a continuous contaminant source term when metals are sorbed to bulk mineral phases. Additional long-term experiments are recommended to definitely rule out irreversible Np(V) sorption behavior at very low surface loadings and environmentally-relevant time-scales.

1. INTRODUCTION

In this study, we investigate the kinetics of neptunium(V) (Np(V)) sorption and desorption on goethite. Neptunium-237 is a radionuclide of concern in nuclear waste repositories due to its long half-life (2.14×10^6 years), toxicity and mobility in oxidizing environments (Thompson, 1982). While initially present in spent nuclear fuel at low levels (0.03%), Np-237 will become the major contributor to the radiation inventory of nuclear waste after approximately 100,000 years (Kaszuba and Runde, 1999). Relative to tetra- and hexavalent neptunium, Np(V) in the form of NpO_2^+ is considered the most relevant and mobile oxidation state in oxic environments (Dozol et al., 1993; Choppin, 2006), and is hence the focus of this study. Goethite (α-FeOOH) is a mineral commonly found in subsurface environments. In addition to their natural abundance, iron (oxyhydr)oxide colloids can potentially form due to the corrosion of waste containers in repositories (Jerden and Kropf, 2007).

* Corresponding author. Present address: Earth Sciences Division, Lawrence Berkeley National Laboratory, 1 Cyclotron Rd., MS 90-1116, Berkeley, CA 94720, USA. Tel.: +1 510 495 8231; fax: +1 510 486 5686.

E-mail address: RMTinnacher@lbl.gov (R.M. Tinnacher).

0016-7037/$ - see front matter © 2011 Elsevier Ltd. All rights reserved.
doi:10.1016/j.gca.2011.08.014

Notation

$[C]_{in}$, $[C]_{out}$ Np(V) concentration in influent or effluent solution (mol L^{-1})
$[C]$ Np(V) solution concentration in flow-cell (mol L^{-1})
ΔG free energy change of reaction
J flow-rate (L min^{-1})
k_+, k_- forward and reverse rate constants for simplified surface reaction
k_2, k_{-2} forward and reverse rate constants for first-order kinetics on site 2 (min^{-1})
K_d sorption distribution coefficient (K_d value) (L g^{-1})
K_{eq} equilibrium constant for surface reaction (in concentration-units)
$K_{eq,1}, K_{eq,2}$ equilibrium constants for reactions on sites 1 and 2 (in concentration-units)
K_F Freundlich coefficient (mol$^{(1-n_1)}$ L^{n_1} g^{-1})
M sorbent/colloid mass in flow-cell (g)
n_1 Freundlich exponent (dimensionless)
Q conditional sorption coefficient for surface reaction (in concentration-units)
Q_1, Q_2 cond. sorption coeff. for reactions on sites 1 and 2 (in concentration-units)
R ideal gas constant
R_+, R_- forward and reverse rates for simplified surface reaction, e.g. (mol (min g)$^{-1}$)
R_{net} net rate of sorption reaction, e.g. (mol (min g)$^{-1}$)
$[S]$ sorbed Np concentration (mol g^{-1})
$[S_1]$, $[S_2]$ Np concentrations sorbed onto sites 1 and 2 (mol g^{-1})
$[S_{Tot}]$ total Np concentration sorbed (mol g^{-1})
T temperature (K)
t time (min)
V_C solution volume in flow-cell (L)
ψ TST-related fitting parameter (dimensionless)
ψ_{ad}, ψ_{de} TST-related fitting parameters for net (ad)sorption/desorption (dimensionless)
ψ_1, ψ_2 TST-related fitting parameters for sites 1 and 2 (dimensionless)

As for other metals, Np sorption to mineral surfaces is an important process controlling contaminant mobility in subsurface environments. On the one hand, Np sorption/desorption onto bulk mineral phases determines the effective removal of dissolved species from the pore water solution and leads to contaminant retardation. On the other hand, Np sorbed onto mobile mineral colloids may remain suspended in solution and can be further transported with the groundwater flow. In both cases, the kinetics of sorption and desorption processes may largely determine the apparent effects of metal surface reactions on contaminant mobility (Saiers and Hornberger, 1996; Cvetkovic, 2000; Missana et al., 2004; Steefel, 2008). However, model calculations including colloid-facilitated transport are especially sensitive to metal sorption/desorption kinetics and the degree of reversibility of the metal-surface binding (Cvetkovic, 2000; Cvetkovic et al., 2004).

For Np(V), previous lab-scale transport studies suggest kinetic limitations for metal sorption/desorption reactions to bulk mineral phases, such as granitic rock (Kumata and Vandergraaf, 1998) and zeolitic tuff (Viswanathan et al., 1998). Furthermore, colloid-facilitated Np transport has been demonstrated on the lab-scale for Np(IV)-bentonite (Nagasaki et al., 1999) and Np(V)–Fe(III) colloid systems (Nagasaki et al., 1994). However, there is little evidence for colloid-enhanced Np mobility on the field scale. For instance, at the Mayak site (Russia) only negligible fractions of Np were found associated with colloidal particles after groundwater filtration with molecular-weight cut-offs of $\geqslant$15 nm (Kalmykov et al., 2007). Hence, in order to assess the potential for colloid-facilitated Np transport under field conditions further, additional research is needed for the characterization of Np(V) desorption behavior, and the development of kinetic modeling concepts.

Results from previous Np(V)–iron (oxyhydr)oxide sorption studies under aerobic conditions indicate a fast initial metal uptake in the order of minutes to hours followed by slower metal sorption rates over days to weeks (Nakayama and Sakamoto, 1991; Kohler et al., 1999; Nakata et al., 2000; Jerden and Kropf, 2007). Neptunium desorption experiments with Fe-(oxyhydr)oxides have been performed at the same chemical solution conditions as during adsorption (Keeney-Kennicutt and Morse, 1984), after controlled changes in solution pH (Nakayama and Sakamoto, 1991; Jerden and Kropf, 2007), or with various types of extraction solutions (Keeney-Kennicutt and Morse, 1984; Nakata et al., 2000; Nakata et al., 2002). Nakata et al. (2000) found that after Np was sorbed to hematite over one week, 24% remained sorbed after sequential desorption steps with 1 M KCl and 0.1 M $K_2C_2O_4$. Keeney-Kennicutt and Morse (1984) observed a Np fraction of approximately 66% desorbed from goethite in deionized water and natural seawater solutions after two hours. Chemical solution conditions during the (ad)sorption step, such as redox conditions and salt composition, affect the extent of metal desorption (Nakata et al., 2002; Jerden and Kropf, 2007). Furthermore, extended (ad)sorption times appear to decrease the reversibility of Np sorption reactions (Nakata et al., 2000).

In addition to the fairly limited number of experimental studies, only a few attempts have been made to simulate Np(V) sorption kinetics based on experimental data. Braithwaite and co-workers (Braithwaite et al., 2000) described Np-237 sorption to a clay-rich sediment over time using 2- and 3-box multi-reaction models, which include fast (equilibrium) and slow reversible sorption sites, as well as one irreversible sorption site. In addition, the kinetics of NpO_2^+ sorption on hydroxyapatite have been simulated

using Lagergren first order kinetics (Thakur et al., 2006). A simulation of Np desorption processes was not included in any of these studies. However, the simulation of kinetically-limited desorption reactions is needed in order to capture contaminant transport behavior over extended time-frames, which is especially important for radionuclides with long half-lives, such as Np-237.

A variety of sorption phenomena can cause differences in contaminant (ad)sorption and desorption behavior leading to an apparent sorption 'asymmetry' depending on the net direction of the surface reaction. They can be summarized as: (1) aging processes, (2) hysteresis effects, and (3) irreversible sorption behavior. As descriptions of these sorption characteristics can vary, we provide the following definitions of these phenomena as they are applied in this study.

For many experimental systems, (ad)sorption rates are significantly higher than desorption rates (McBride, 1991), which can be explained by differences in activation energies between forward and reverse reactions (Adamson, 1990; Lasaga, 1998). However, if sorption rates appear to change over extended time-frames, 'aging processes' may be involved. In this study, 'aging' is defined as one or more surface chemical process(es) that follow(s) the initial sorption reaction and cause(s) changes in contaminant surface speciation over time (Nyffeler et al., 1984; Jannasch et al., 1988; Comans et al., 1991; Millward and Liu, 2003; Garnier et al., 2006). Hence, a fraction of metal surface species may become less 'accessible' for a rapid equilibration with the solution phase (Smith et al., 2009; Wendling et al., 2009) resulting in lower metal desorption rates and/or a contaminant fraction that remains sorbed within experimental time-frames. Overall, aging is a time-dependent phenomenon that may or may not result in apparent irreversible sorption behavior or sorption hysteresis.

In contrast to aging, we define sorption 'hysteresis' as a thermodynamic property, which is indicated by different sorption affinities depending on the net *direction* of surface reactions, i.e. during net (ad)sorption and desorption processes (Sander et al., 2005). This results in different isotherms and sorption equilibria for (ad)sorption and desorption processes, and creates a hysteresis loop (Fig. 1a). Systems with sorption hysteresis are believed to exhibit different microscopic pathways for metal uptake and release (Sander et al., 2005).

In the literature, the term hysteresis is often used as an equivalent to some degree of irreversible sorption behavior, which implies a non-equilibrium transfer of contaminants between solution phase and mineral surfaces (e.g., (Laird et al., 1994; Gao et al., 2003; Sander et al., 2005)). Under constant solution conditions, the contaminant fraction that remains sorbed after desorption equilibration is often larger than the one during the initial (ad)sorption step. This difference is commonly interpreted as an 'irreversibly' sorbed fraction (shown as fraction A in Fig. 1a). However, strictly speaking, irreversible sorption represents only one specific case of sorption hysteresis (Sing et al., 1985), where a fraction of the contaminant remains sorbed (or is expected to do so) after complete desorption equilibration with a solute-free solution of identical chemical composition (fraction B in Fig. 1a). Whenever we state the term irreversible sorption, we refer to this latter, strict definition (fraction B).

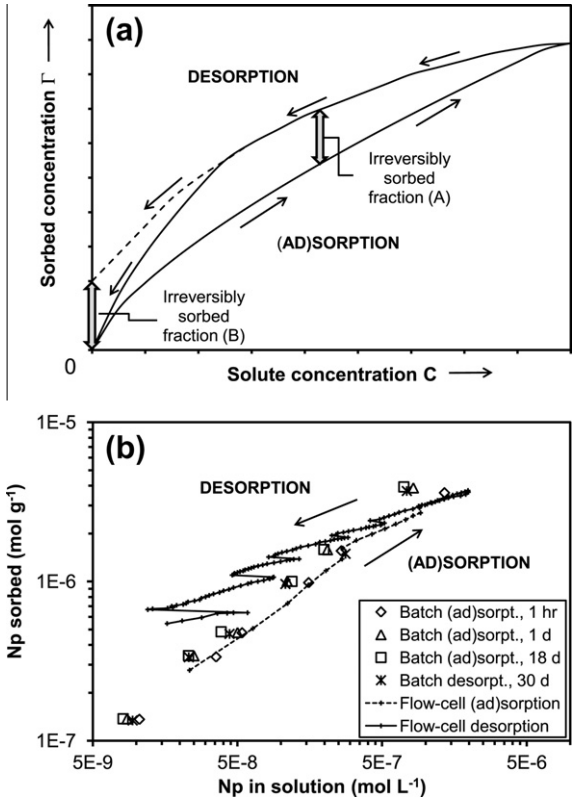

Fig. 1. (a) Qualitative concept of sorption hysteresis at 'true' equilibrium conditions, where (ad)sorption and desorption processes show different sorption isotherms. A larger concentration remaining sorbed after desorption is commonly interpreted as 'irreversibly' sorbed fraction (A). But following a strict definition (Sing et al., 1985), a contaminant fraction is only irreversibly sorbed, if the hysteresis loop cannot be closed (B). (b) Np (ad)sorption/desorption isotherms determined in batch and flow-cell experiments at the same chemical solution conditions (pH = 8, I = 5 mM NaCl/0.7 mM $NaHCO_3$): a strictly-defined, irreversible Np sorption cannot be evaluated within the scope of the flow-cell experiment.

Varying approaches have been used in the literature for the interpretation and simulation of aging and hysteresis. Aging processes are often interpreted based on an increase in apparent distribution coefficients (K_d values) over time, and the need to incorporate consecutive surface sites into kinetic sorption models (Nyffeler et al., 1984; Jannasch et al., 1988; Ciffroy et al., 2001; Ciffroy et al., 2003; Garnier et al., 2006). Hysteresis effects have been quantified based on empirical hysteresis indices, which parameterize observed differences in experimental adsorption and desorption data (e.g., (Laird et al., 1994; Huang and Weber, 1997; Lesan and Bhandari, 2003)). A detailed overview of these parameters is given elsewhere (Sander et al., 2005); however, the area (Fig. 1a) between adsorption and desorption isotherms (Zhu and Selim, 2000) and changes in apparent K_d values (Laird et al., 1994; Huang et al., 1998) are some examples of sorption characteristics compared

in hysteresis indices. In kinetic sorption models, hysteresis has mostly been simulated indirectly, by including a variety of surface site types with fast (or equilibrium) and slow (or 'irreversible') sorption kinetics (Buchter et al., 1996; Zhu and Selim, 2000; Undabeytia et al., 2002; Selim and Zhu, 2005).

Changes in apparent distribution coefficients and other sorption parameters as a function of time or reaction direction may be good indications for aging and hysteresis effects, but do not provide any predictive capabilities. Furthermore, the interpretation of a strictly-defined irreversible sorption behavior based on experimental 'short-term' data, e.g., observed over weeks, seems inappropriate, especially if contaminant transport predictions extend over substantially longer time-frames. Most currently available kinetic models incorporate fundamental changes in (ad)sorption and desorption behavior indirectly. However, we believe that a new approach is needed that allows for a direct simulation of changes in sorption reaction pathways, e.g., as a function of the direction of surface reactions.

The goal of this study is to improve the understanding of Np(V) sorption and desorption kinetics on goethite by combining experimental data with kinetic modeling. In particular, the relevance of the following (kinetic) sorption characteristics is evaluated: (1) aging processes, (2) hysteresis effects, and (3) equilibrium versus irreversible sorption behavior. The proposed modeling concept and general results should be applicable to many other metal-mineral systems besides Np and goethite.

2. MATERIALS AND METHODS

2.1. Experimental

2.1.1. Goethite preparation and characterization

Unless stated otherwise, all solutions were prepared with ultrapure water (Milli-Q Gradient System, >18 MΩ cm resistivity) using ACS grade chemicals without further purification. Goethite (α-FeOOH) was synthesized from $Fe(NO_3)_3 \cdot 9H_2O$ as described in the literature (Schwertmann and Cornell, 1991); for details see Electronic Annex. A XRD pattern confirmed goethite as the major phase (Scintag PAD-V diffractometer; ICDD reference card 29-0713). A point of zero salt effect of 8.5 ± 0.1 was determined through potentiometric titrations of 10 g L^{-1} goethite suspensions in 0.001 M, 0.01 M, and 0.10 M NaCl (Metrohm titrator, room temperature, Ar(g) headspace). Potential changes in goethite particle size and morphology due to continuous stirring in flow-cell experiments were evaluated based on BET surface area measurements (Micrometrics Gemini surface area analyzer) and scanning electron microscope images (JEOL JSM-7401F SEM). There was no significant difference in the BET surface area of goethite before (14.8 m^2 g^{-1}) and after (13.5 m^2 g^{-1}) stirring based on a 99.9% confidence limit. However, SEM analysis indicated the destruction of star-shaped particles over time, which could generate small amounts of fresh, reactive surface sites (Fig. EA-1, Electronic Annex). These morphological changes were not included in kinetic sorption models, as we assumed a large excess of total reactive surface sites, and as potential changes in site concentrations or distributions could not be specifically quantified based on BET measurements. However, future studies may benefit from a more detailed characterization of potential changes in surface site densities over long experimental time-frames, e.g. using mineral titrations.

2.1.2. Composition and analysis of solutions

A 1.5 mM $^{237}Np(V)$ stock solution was purified by anion exchange to remove the ^{233}Pa daughter, then used to prepare a 3.2 μM ^{237}Np working solution in 5 mM NaCl/0.7 mM $NaHCO_3$ (pH 8). An aliquot of a tritium (^3H) stock solution was added to achieve a non-reactive tracer concentration of 1000 cpm ml^{-1}. In order to ensure equilibration with atmospheric $CO_2(g)$, the solution was stirred uncapped for more than 3 days prior to use. Over the course of the experiment, ^{237}Np and ^3H concentrations were determined by liquid scintillation analysis (Packard Tricarb 2550TR/XL LSC). Pure ^{237}Np and ^{233}Pa solutions were used to select an appropriate alpha/beta discrimination setting for liquid scintillation counting. No specific measures were taken to prevent bacterial growth in experimental solutions or the flow-cell setup.

2.1.3. Setup for flow-cell experiment

A flow-cell design was used to characterize Np(V) sorption/desorption kinetics on goethite under controlled chemical conditions. Flow-cell experiments provide several advantages compared to batch systems, such as continuous sampling and removal of desorbed reaction products, an increased total solute mass in contact with the mineral surface, and the minimization of mass transfer limitations in terms of film or particle diffusion (Seyfried et al., 1989; Selim and Amacher, 1997). In addition, flow-cell experiments allow for variations in solute–solid contact times over the course of an experiment based on controlled changes in flow rates (Limousin et al., 2007) or flow interruptions (stop-flow events). These features can be used to evaluate kinetically-limited processes over the course of an experiment, e.g. as a function of surface loading and time.

Flow-cell experiments were set up in a 10 ml ultra-filtration stirred cell (Millipore; fitted with 100 nm pore size Millipore polycarbonate filter). The influent flow-rate was set at 12 ml h^{-1} (Minipuls 2 peristaltic pump) resulting in an average retention time of 50 min. The assumption of ideal mixing conditions in the flow reactor was confirmed by comparing measured tritium break-through with the analytical solution for the given average retention time (data not reported). Effluent fractions were collected on an Eldex fraction collector over time, and their exact volumes determined gravimetrically.

Initially, goethite and background electrolyte were loaded into the flow-cell to generate 10 ml of a 2 g L^{-1} suspension, and equilibrated over a time-frame equivalent to approximately 50 reactor pore volumes. The '(ad)sorption step' of the experiment was started by pumping Np(V) working solution (3.2 μM ^{237}Np, 5 mM NaCl/0.7 mM $NaHCO_3$, pH 8, 1000 cpm ml^{-1} ^3H) into the flow-cell. In order to determine if sorption was rate-limited under flow conditions, the flow

was stopped twice for time-intervals of 1.95 and 21.1 h, respectively while continuously stirring the suspension. This effectively changed the solute–solid contact time from the average retention time in the reactor (50 min) to the individual time-periods of the stop-flow events.

After sorption of Np(V) on goethite over 26.38 h (1.10 days, 3.995 pore volumes exchanged), a 'desorption step' was initiated by pumping Np- and tritium-free background electrolyte solution into the cell. In between the sorption and desorption phases a third (ad)sorption stop-flow event occurred for 0.53 h. The desorption part of the experiment was performed in the same manner as the (ad)sorption step (over 32.46 days) except for the differences in influent solution composition. Additional stop-flow events of increasing time-length (20.63, 66.20, 87.58, 138.02 and 413.45 h) were performed to characterize potential rate limitations for Np(V) desorption from goethite. The total time-frame of the flow-cell experiment was 33.56 days.

2.1.4. Setup for Batch Experiments

Batch experiments were performed to compare Np(V) sorption/desorption behavior in batch and flow-cell systems at the same chemical solution conditions but different sorption equilibration times. For the batch (ad)sorption step, goethite was equilibrated with various concentrations of Np(V) in centrifuge vials while mixing on an overhead shaker ($2\ g\ L^{-1}$ α-FeOOH, pH 8, $I = 5$ mM NaCl/0.7 mM $NaHCO_3$, atmospheric CO_2). At selected time-points, 1.1 ml-fractions of the suspensions were removed, centrifuged at 8000 rpm over 60 min (Beckman-Coulter Allegra 22-R, F2404 rotor), and the resulting supernatant solutions analyzed for remaining metal concentrations. After Np(V) sorption over 18 days, the remaining sample suspensions were centrifuged (4500 rpm for 60 min; swing-bucket rotor SX-4250) and the supernatant solutions replaced with fresh background electrolyte of the same chemical solution composition. After metal desorption under shaking over 30 days, Np solution concentrations were determined as described for the (ad)sorption step above.

2.2. Modeling

Our modeling goal is to simulate the kinetic Np(V) adsorption/desorption behavior observed in the flow-cell system with a 'global' set of fitting parameters that is valid for both sorption directions. In the process of model development, we evaluated the relevance of (1) aging, (2) hysteresis, and (3) irreversible sorption behavior. In the following, we provide a general overview of our modeling approach; additional details are given in Section 3.2 Modeling Results.

The simulation of Np(V) solution concentrations over time is based on the combination of the metal mass balance equation for the flow-cell with a kinetic rate law describing Np sorption reactions. The Np mass balance in the flow-cell is defined as (Bar-Tal et al., 1990; Seyfried et al., 1989)

$$[C]_{in}J = [C]_{out}J + V_C\frac{d[C]}{dt} + M\frac{d[S]}{dt} \quad (1)$$

with $[C]_{in}$, $[C]_{out}$ = Np(V) concentration in influent or effluent solution (mol L^{-1}), $[C]$ = Np(V) solution concentration in flow-cell (mol L^{-1}), J = flow-rate (L min^{-1}), t = time (min), V_C = solution volume in flow-cell (L), M = sorbent/colloid mass in flow-cell (g), and $[S]$ = sorbed concentration (mol g^{-1}).

As ideal mixing conditions in the flow-reactor were demonstrated experimentally using a non-reactive tracer (comparison between experimental and mathematical data not reported), we can define $[C] = [C]_{out}$ and rearrange the mass balance equation to

$$\frac{d[C]}{dt} = \frac{1}{V_C}\left\{([C]_{in} - [C])J - M\frac{d[S]}{dt}\right\} \quad (2)$$

Numerical solutions for metal concentrations ($[C]$) at individual time steps were calculated based on a finite difference approach (Euler method). Fortran codes (Silverfrost Plato 4.10 compiler) were combined with PEST (Parameter ESTimation), a non-linear parameter estimation program, which determines fitting parameters by least square minimization utilizing the Gauss–Marquardt–Levenberg method (Doherty, 2004). For the non-linear fitting in PEST, data points were solely weighted based on their individual analytical errors for Np liquid scintillation analysis (In PEST: *Weight = 1/absolute error*).

For testing of various modeling concepts, different expressions of reversible sorption rate laws were substituted for $d[S]/dt$ in Eq. (2) (Skopp and McCallister, 1986; Bar-Tal et al., 1990). Overall rate laws were described by Np(V) sorption to surface 'sites' based on kinetic isotherm expressions, which were selected from linear, Langmuir or Freundlich equations (Table 1). Traditionally, metal sorption reactions on iron-oxide minerals have been simulated assuming two types of mineralogical surface sites with high (type 1) and low (type 2) sorption affinities (Dzombak and Morel, 1990). While high- and low-affinity surface sites may have some kinetic relevance as well, we will use the term 'site' in context of our kinetic modeling in a much broader sense. Following 'multi-reaction' modeling approaches by Selim and Amacher (1997), a 'site' represents any type of sorption/desorption interaction between solutes and the mineral phase that can be differentiated by their specific kinetic behavior or their degree of sorption non-linearity. Numerous retention mechanisms and processes may be occurring in parallel or consecutively for the Np(V)–goethite system under investigation. However, this multi-reaction modeling approach does not require any knowledge of exact sorption/retention mechanisms a priori, and allows for the testing of various configurations of surface 'sites'.

The relevance of various (kinetic) sorption characteristics for Np(V) sorption/desorption on goethite was evaluated as follows. First, aging processes were interpreted based on the necessity to include two or more site types (Fig. 2), e.g., with different kinetic sorption characteristics (Ciffroy et al., 2001; Ciffroy et al., 2003; Garnier et al., 2006). Second, the significance of sorption hysteresis and 'irreversible sorption' was determined based on (1) a comparison of 'overall' Np(V) distribution coefficients (K_d values) calculated from kinetic parameters, which were fitted to net (ad)sorption and desorption data separately; and (2) the improvement of model fits after the incorporation of an irreversible sorption site (Buchter et al., 1996; Celis and Koskinen, 1999).

Table 1
Sorption isotherms used in kinetic modeling.

Sorption isotherm	Rate law: $R_{net} = R_+ - R_-$	Equilibrium equation
Linear (1st order)	$d[S]/dt = k_+[C] - k_-[S]$	$[S] = (k_+/k_-)[C] = K_d[C]$
Langmuir	$d[S]/dt = k_+[C]([S]_{max} - [S]) - k_-[S]$	$[S] = \frac{(k_+/k_-)[S]_{max}[C]}{1+(k_+/k_-)[C]} = \frac{K_L[S]_{max}[C]}{1+K_L[C]}$
Freundlich	$d[S]/dt = k_+[C]^n - k_-[S]$	$[S] = (k_+/k_-)[C]^n = K_F[C]^n$
Empirical	$d[S]/dt = k_+[C]^a - k_-[S]^b$	$[S] = (k_+/k_-)^{1/b}[C]^{a/b}$

$[S]$ = sorbed conc. (mol g^{-1}), $[C]$ = solution conc. (mol L^{-1}), k_+ = forward rate constant, k_- = reverse rate constant, *n, a, b* = sorption coefficients (), K_d = distribution coefficient (L g^{-1}), K_L, K_F = Langmuir (L mol^{-1}), Freundlich const. ($mol^{(1-n)}L^n g^{-1}$).
Note: Units of rate constants vary depending on individual rate law and the correction of unit differences between solution and surface concentrations.

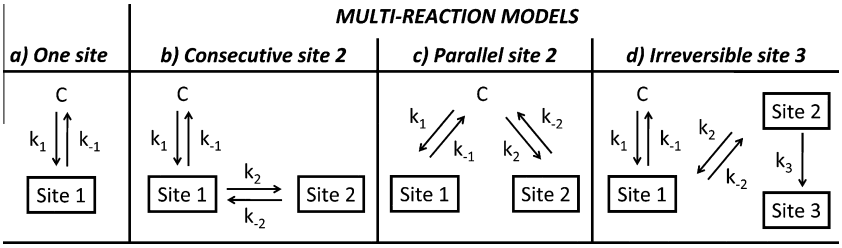

Fig. 2. Examples of conceptual models used for the simulation of Np(V) sorption/desorption kinetics to goethite in 1-site and multi-reaction models. In all models, site 1 represents a non-linear equilibrium site (Freundlich or Langmuir). In 2-site consecutive models (b), site 2 is described by reversible first-order sorption kinetics; in 2-site parallel models (c), site 2 shows the same isotherm kinetics as site 1. Metal transfer to the irreversible site 3 (d) follows (irreversible) first-order kinetics.

Last, we evaluated the possibility of different net (ad)sorption and desorption rates in the absence of irreversible sorption characteristics, which allows for a differentiation between Np(V) equilibrium sorption and irreversible sorption behavior. For this purpose, we introduced a kinetic modeling concept related to transition state theory (also known as activated complex theory), which is based on the following general considerations. For net (ad)sorption and desorption processes, the same overall sorption reaction may occur via different reaction pathways. For instance, metal uptake may be a combination of chemical and physical processes, such as various types of diffusion and chemical surface reactions, while desorption is more likely to be dominated by physical processes (Jannasch et al., 1988; Sparks, 2000). Furthermore, aging processes can affect metal speciation on the surface over time (Comans et al., 1991; Ciffroy et al., 2001) resulting in the formation of different reaction intermediates for net (ad)sorption and desorption processes. According to transition state theory (TST), variations in reaction pathways lead to changes in apparent activation energies and overall reaction rates (Lasaga, 1998). For example, experimentally-determined activation energies for contaminant sorption/desorption reactions have been previously used to gain insights into overall reaction mechanisms (Ogwada and Sparks, 1986b; Farrell et al., 1999), and to evaluate differences between net (ad)sorption and desorption processes (Ogwada and Sparks, 1986a). Hence, a TST-related modeling concept allows us to link differences in net (ad)sorption and desorption rates to variations in overall reaction pathways without assuming hysteresis effects or irreversible sorption behavior a priori. Similar kinetic concepts have been applied to characterize the kinetics of environmentally relevant aqueous solution reactions (Morgan and Stone, 1985), gas adsorption on solids (Adamson, 1990), and mineral dissolution/precipitation reactions for various minerals (Alekseyev et al., 1997; Carroll et al., 1998; Oelkers, 2001; Chairat et al., 2007; Dixit and Carroll, 2007; Yang and Steefel, 2008; Maher et al., 2009). However, these modeling concepts have not been utilized for contaminant sorption onto mineral surfaces previously.

3. RESULTS AND DISCUSSION

3.1. Experimental results

3.1.1. Results from flow-cell experiment

In the following, we present experimental and modeling results by depicting solution concentrations of Np(V) and tritium in the flow-cell effluent as a function of pore volumes exchanged (Fig. 3). The number of pore volumes is an equivalent of time under flow conditions, but remains constant during stop-flow events.

At the beginning of the (ad)sorption step, an influent with a constant Np(V) concentration (3.2 μM ^{237}Np) is pumped into the metal-free system. Due to mixing and dilution in the cell, this causes a slow increase in Np(V) effluent concentrations over time (Fig. 3). Furthermore, Np(V) is 'lost' from solution due to metal sorption to goethite, which is indicated by lower Np(V) effluent concentrations compared to the tracer. When the influent flow was stopped and resumed for (ad)sorption stop-flow events, Np(V) concentrations in the effluent remained fairly constant. This suggests that Np(V) (ad)sorption was close to steady-state

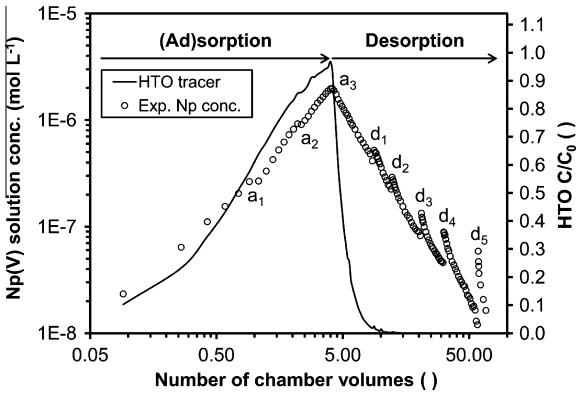

Fig. 3. Experimental results from Np(V)–goethite flow-cell experiment performed at: 3.16×10^{-6} M ((ad)sorption) and 0 M (desorption) Np(V) influent concentrations, 2 g L^{-1} goethite, pH = 8, $I = 5.7 \times 10^{-3}$ M NaCl/$NaHCO_3$, in 10 ml flow-cell solution volume, with a 0.2 ml min^{-1} flow-rate (50 min. average retention time); adsorption stop-flow events took: $a_1 = 1.95$ h, $a_2 = 21.1$ h, $a_3 = 0.53$ h; desorption stop-flow events: $d_1 = 20.63$ h, $d_2 = 66.20$ h, $d_3 = 87.58$ h, $d_4 = 138.02$ h, $d_5 = 413.45$ h.

under flow conditions (average retention time of 50 min) and for the given surface loadings (1.62 and 2.90 μmol Np_{sorbed} g^{-1} goethite for the first and second stop-flow events).

The desorption step was initiated by switching to a Np-free influent solution after pumping Np(V) working solution into the flow-cell for approximately four (3.995) pore volumes (total (ad)sorption contact time of 26.38 h). This lead to a decrease in Np(V) and tritium concentrations in the effluent. After exchanging 5.7 pore volumes of electrolyte, the relative ^3H concentration in the effluent reached approximately 2% of the relative tracer concentration present at the beginning of the desorption step. This is consistent with the expected behavior of a non-reactive tracer. Neptunium(V) effluent concentrations remained higher compared to the tracer due to Np(V) desorption from goethite. During the desorption process, the flow-cell was stopped five times (20.63, 66.20, 87.58, 138.02 and 413.45 h) to evaluate kinetic limitations for metal desorption reactions at various time-points and over an approximately one order of magnitude range of surface loadings (from 3.73 to 0.54 μmol Np_{sorbed} g^{-1}goethite). The increases in Np effluent concentrations following each stop-flow event indicate that additional metal desorption occurred under extended desorption equilibration times. Therefore, experimental data suggest that steady-state conditions were not reached under continuous flow conditions, and that Np desorption is rate-limited within an average retention time of 50 min.

We calculated a decrease in Np surface loads from 7% to 1% (3.73 and 0.54 μmol Np_{sorbed} g^{-1}goethite) over the course of the desorption step assuming an average site density of 2.3 sites nm^{-2} for iron oxides (Dzombak and Morel, 1990). When examining Np(V) sorption to hematite, Kohler and co-workers (1999) noted that for adsorption densities above 5% of the total site concentration, the slope of sorption isotherms decreased below one, which indicates Np(V) interactions with weaker sorption sites. Hence, our experimental results may be indicative of the influence of high- and low-affinity surface sites, as defined by Dzombak and Morel (1990).

After passing 68 pore volumes through the flow-cell, 15% of the initial Np remained sorbed to goethite, and Np was continuously desorbed until the termination of the experiment. Hence, based on experimental results alone, it is unknown whether a complete recovery of sorbed Np could have been achieved. Slow Np desorption may be the result of Np(V) partitioning to strongly sorbing sites with considerably slower desorption kinetics. Nevertheless, slow desorption reactions do not necessarily imply irreversible Np sorption (Fig. 1a). The development of a kinetic sorption/desorption model allows a detailed evaluation of this question.

3.1.2. Results from batch experiments

Results from batch (ad)sorption/desorption experiments are presented in the form of Np(V) sorption/desorption 'isotherms' (Fig. 1b). This allows a comparison of metal sorption behavior in batch and flow-cell systems at the same chemical solution conditions but different sorption equilibration times. However, due to kinetic limitations, portions of these 'isotherms' do not represent full equilibrium conditions for Np surface reactions.

For metal (ad)sorption in batch systems, there is no indication for surface site limitations over the range of neptunium surface concentrations tested. Furthermore, aqueous Np(V) concentrations decrease only slightly when sample equilibration times are extended from one hour to one day. This indicates that steady-state conditions have nearly been achieved within a one-hour time-frame. Flow-cell data based on a 50-min average retention time match the one-hour batch (ad)sorption isotherm quite well, except for the highest metal concentration tested. Apparently, steady-state conditions are not reached within a one-hour time-frame at high surface loadings (3.73 μmol Np_{sorbed} g^{-1}goethite). For the metal desorption step, Np partitioning between solid and solution phases deviates substantially between flow-cell and batch systems. Under flow conditions, net Np desorption rates are not sufficiently fast to reach equilibrium solution concentrations in the cell. The system continuously moves away from the steady-state conditions that are indicated by batch (ad)sorption/desorption results. When Np equilibration times are substantially increased during desorption stop-flow events (20.63–413.45 h), aqueous Np concentrations increase and approach batch desorption isotherms. Overall, data indicate that steady-state conditions for Np (ad)sorption and desorption are reached within one and 30 day(s), respectively.

(Ad)sorption/desorption 'isotherms' from the flow-cell system further suggest that 'true' hysteresis effects are probably minimal. Apparent hysteresis effects, interpreted based on the differences between the (ad)sorption and desorption 'isotherms', may be primarily due to kinetic limitations and short Np desorption equilibration times under flow conditions. In addition, the comparison of experimental results with a theoretical example of metal sorption/desorption behavior shows that the flow-cell experiment was not

performed long enough to evaluate a strictly-defined irreversible sorption behavior (fraction B in Fig. 1a). This is due to the continuous, slow Np desorption processes that were observed until the end of the experiment. As a consequence, an interpretation of irreversible sorption behavior based on modeling results is limited to the time-frames and system conditions evaluated in the flow-cell experiment.

3.2. Modeling results for flow-cell experiments

In this section, we first describe the main characteristics of the kinetic multi-reaction model that provides the best model fit using a minimum number of fitting parameters. This is followed by a brief, general overview of the mathematical background for transition state theory (TST), and a discussion of the incorporation of the TST-based concept into the model framework. Additional information regarding TST can be found in the Electronic Annex and in the literature (Morgan and Stone, 1985; Stumm, 1992; Lasaga, 1998; Brantley, 2008). Furthermore, the Electronic Annex also contains a description of Np(V) (ad)sorption and desorption kinetics on goethite in batch systems, as predicted from the best model fit of experimental flow-cell data. Finally, we present an evaluation of the specific model features that are relevant for the interpretation of kinetic sorption characteristics.

3.2.1. Main characteristics of kinetic multi-reaction model

Within the scope of this study, a multi-reaction Freundlich model provides the best model fit with the lowest number of fitting parameters (Fig. 4; Table 2). This model includes two surface 'sites' set up in series (Fig. 2b), and allows for changes in sorption rates depending on the net direction of surface reactions based on a TST-related modeling concept. Both sites are treated as 'unlimited' surface sites, as no specific surface site concentrations are included in the model. Site 1 simulates the direct sorption of aqueous Np(V) to the surface in form of a non-linear, Freundlich-isotherm-based equilibrium site

$$[S_1] = K_F[C]^{n_1} \tag{3}$$

where $[C]$ and $[S_1]$ are the respective Np(V) concentrations in solution (mol L^{-1}) and sorbed onto site 1 (mol g^{-1}), K_F represents the Freundlich coefficient (mol$^{(1-n_1)}$ L^{n_1} g^{-1}), and n_1 the Freundlich exponent (dimensionless). Site 2 describes the slow (kinetically-controlled), consecutive transfer of sorbed Np from site 1 to site 2, which is simulated with a first-order rate law.

$$\frac{d[S_2]}{dt} = k_2[S_1] - k_{-2}[S_2] \tag{4}$$

In this equation, k_2 and k_{-2} represent the forward and reverse rate constants (min^{-1}), $[S_2]$ is the Np surface concentration on site 2 (mol g^{-1}), and t time (min). Based on model testing (data not reported), Np sorption onto goethite appears to be strongly non-linear for the forward reaction to site 1 under the given experimental conditions. We selected a Freundlich isotherm for site 1, as batch sorption data do not indicate any substantial surface site limitations in form of a 'plateau' of metal surface concentrations

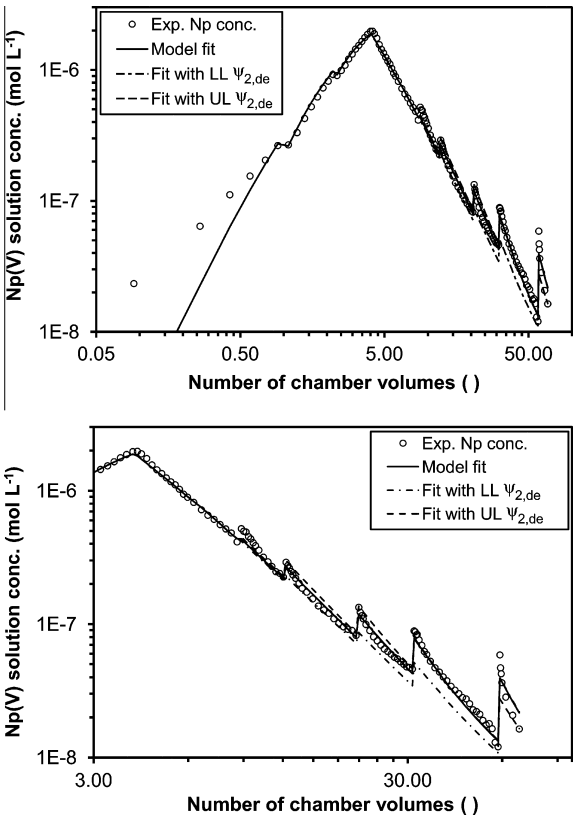

Fig. 4. Best model fit with minimum number of fitting parameters: multi-reaction model including an equilibrium Freundlich site (site 1), a consecutive first-order site (site 2) and the fitting parameter $\psi_{2,de}$. Dashed lines represent calculated model outputs using the upper ($UL = 1.62 \times 10^{-2}$) and lower limit ($LL = 3.75 \times 10^{-3}$) values of $\psi_{2,de}$. Model fits overlap in regions where individual lines are not visible.

(Fig. 1b), which is typical for Langmuir isotherms. Linear isotherms were not able to capture Np sorption/desorption behavior ('curvature') to goethite appropriately; empirical-isotherm models (Bar-Tal et al., 1990) including non-linear kinetics for the reverse reaction (Table 1) could not improve model fits any further. Equilibrium or 'instantaneous' sorption on site 1 was confirmed mathematically as described in detail in the Electronic Annex (Fig. EA-2).

Differences in reaction rates between net (ad)sorption and desorption conditions became apparent during model development. These differences can be simulated by treating the (ad)sorption and desorption parts independently, which is a common practice for the interpretation of hysteresis effects (Huang and Weber, 1997; Lesan and Bhandari, 2003; Missana et al., 2004; Shirvani et al., 2006). In these 'split' models, two sets of kinetic rate constants are used as fitting parameters depending on the net direction of surface reactions. However, this effectively doubles the number of fitting parameters and impedes our goal of producing a 'global' model. Therefore, a TST-related kinetic concept was introduced to simulate variations in (ad)sorption and desorption rates on site 2. The resulting best-model-fit is based on a 'global' set of fitting parameters except for the

Table 2
Model fitting parameters for Freundlich 1-site and 2-site multi-reaction models.

Fitting parameters	Units	Freundlich 1-site (global)	Freundlich 2-site (global)	Freundlich 2-site (split)		Freundlich 2-site (global) with $\psi_{2,de}$[d]
				(Ad)sorption	Desorption	
K_F	$(mol^{(1-n_1)}\ L^{n_1}\ g^{-1}$	1.48E-04	1.52E-03	2.80E-04	2.08E-04	1.07E-03
K_F-LL[a]	$(mol^{(1-n_1)}\ L^{n_1}\ g^{-1}$	1.03E-04	8.93E-04	1.70E-04	1.48E-04	1.39E-03
K_F-UL[b]	$(mol^{(1-n_1)}\ L^{n_1}\ g^{-1})$	2.13E-04	2.59E-03	4.61E-04	2.93E-04	8.20E-04
n_1	()	0.33	0.46	0.35		0.45
n_1-LL	()	0.31	0.42	0.31		0.43
n_1-UL	()	0.36	0.50	0.39		0.47
k_2	(min^{-1})	n/a	1.50E-04	5.16E-03	4.21E-06	5.03E-03
k_2-LL	(min^{-1})	n/a	1.10E-04	2.67E-03	3.19E-08	2.87E-03
k_2-UL	(min^{-1})	n/a	2.03E-04	9.94E-03	5.55E-04	8.82E-03
k_{-2}	(min^{-1})	n/a	2.93E-04	1.33E-02	6.07E-05	1.22E-02
k_{-2}-LL	(min^{-1})	n/a	2.22E-04	6.61E-03	4.66E-05	6.29E-03
k_{-2}-UL	(min^{-1})	n/a	3.87E-04	2.67E-02	7.89E-05	2.37E-02
$\psi_{2,de}$	()	n/a	n/a	n/a	n/a	9.96E-03
$\psi_{2,de}$-LL	()	n/a	n/a	n/a	n/a	3.75E-03
$\psi_{2,de}$-UL	()	n/a	n/a	n/a	n/a	1.62E-02
GOF value[c]	$(mol\ L^{-1})^2$	3.68E-12	2.13E-12	7.30E-13		9.81E-13
Correlat. factor	()	0.9533	0.9667	0.9881		0.9842

[a] LL = lower limit for fitting parameter (95% confidence limit).
[b] UL = upper limit for fitting parameter (95% confidence limit).
[c] GOF value = Goodness-of-fit value (sum of squared weighted residuals).
[d] Considered the best model fit with a minimum number of fitting.

TST-related parameter ψ_2, which varies for net (ad)sorption and desorption conditions.

3.2.2. General background for transition state theory-related modeling concept

Transition state theory provides a direct link between the rate and the driving force of a reaction. In an elementary reaction, reactants are first transformed into an activated complex before they form the reaction products (Brantley, 2008). The bimolecular rate constant (k) for this elementary process is dependent on its associated activation energy (E_0), which is the difference in potential energy between reactants and the activation complex (Stumm, 1992; Lasaga, 1998).

For a fixed set of chemical solution conditions in the flow-cell experiment, we neglect solution speciation and assume the following, simplified surface reaction for illustration purposes.

$$C \underset{k_-}{\overset{k_+}{\rightleftharpoons}} S \tag{5}$$

Forward (R_+) and reverse (R_-) rates are commonly expressed in units of concentrations in the kinetics literature (Lasaga, 1998). For Eq (5), they are defined as

$$R_+ = k_+[C] \tag{6a}$$

and

$$R_- = k_-[S] \tag{6b}$$

where k_+ and k_- are forward and reverse rate constants. Based on the principle of detailed balancing, both rates are equal for elementary reactions under equilibrium conditions (Lasaga, 1998). Hence, the equilibrium constant for the surface reaction is

$$K_{eq} = \frac{k_+}{k_-} = \frac{[S]_{eq}}{[C]_{eq}} \tag{7}$$

We now introduce the conditional sorption coefficient Q, which is the ratio of sorbate and solution concentrations under non-equilibrium conditions. We define Q in accordance with existing environmental chemistry nomenclature (Stumm, 1992), which describes equilibrium constants for surface reactions K_{eq} as (ad)sorption constants. (In contrast, Q is commonly defined as aqueous ion activity quotient in mineral dissolution/precipitation studies applying TST-related kinetic concepts (Alekseyev et al., 1997; Carroll et al., 1998)).

Based on the relationship between kinetics and thermodynamics (see Electronic Annex), the ratio of the forward (R_+) and reverse (R_-) rates of an elementary reaction can be expressed as (Morgan and Stone, 1985; Stumm, 1992)

$$\frac{R_+}{R_-} = \frac{K_{eq}}{Q} = \exp\left(-\frac{\Delta G}{RT}\right) \tag{8}$$

where ΔG is the free energy change (driving force) of the reaction, R the ideal gas constant and T temperature (K). From Eq. (7), the net rate of the sorption reaction ($R_{net} = R_+ - R_-$) follows as

$$R_{net} = k_+[C]\left(1 - \exp\left(\frac{\Delta G}{RT}\right)\right) = k_+[C]\left(1 - \frac{Q}{K_{eq}}\right) \tag{9}$$

From a thermodynamic point of view, Eq. (7) is only valid if the equilibrium constant and conditional sorption coefficient are expressed in units of activities. However, the end result (Eq. (8)) remains the same when an activity correction is included, as activity coefficients are canceled for the ratio of Q/K_{eq} (for details see Electronic Annex).

This rate law describes a direct relationship between the driving force (ΔG) and the net rate of an elementary reaction based on the breakdown of a single critical activation complex (Lasaga, 1998; Chairat et al., 2007; Brantley, 2008). Strictly speaking, kinetic expressions based on TST concepts are only valid for elementary reactions (Brantley, 2008). However, this concept may be applied to overall reactions if one assumes that the overall reaction mechanism, consisting of a series of elementary reactions, is primarily rate-limited by one single elementary reaction (Lasaga, 1998). Otherwise, Eq. (8) should be regarded as a semi-empirical relationship describing the net kinetic rate of an overall reaction.

A more general form of the TST rate law formulation, which has been applied to overall reactions in the past (Morgan and Stone, 1985; Carroll et al., 1998; Maher et al., 2009) is

$$R_{net} = R_+\left(1 - \left(\frac{Q}{K_{eq}}\right)^{\psi}\right) = R_+\left(1 - \exp\left(\frac{\psi \Delta G}{RT}\right)\right) \qquad (10)$$

Generally, the variable ψ should be interpreted as an empirical fitting parameter. However, in some instances it may also be regarded as the inverse ratio of the Temkin coefficient, which is the average stoichiometric number of activation complexes formed per reactant (Oelkers, 2001; Chairat et al., 2007; Dixit and Carroll, 2007). For example, with a ψ value of 0.5 and a Temkin coefficient of 2, two moles of activation complexes are generated per mol of reactants. Hence, a deviation of ψ from unity has been interpreted as an indication for the involvement of a number of parallel and/or successive elementary reactions with comparable rates (Alekseyev et al., 1997). On the other hand, at $\psi = 1$, TST-related rate laws become mathematically equivalent to their corresponding isotherm-based rate laws (Table 1).

We expanded this TST-related concept further to allow for different apparent activation energies and reaction rates for the overall sorption processes depending on the *net direction* of a surface reaction, i.e. (ad)sorption versus desorption. Hence, changes in sorption rates are assumed to be due to different reaction pathways depending on the net direction of sorption reactions. In this semi-empirical approach, the parameter ψ (Eq. (9)) is fitted individually for each direction: one value of ψ is calculated for net adsorption at $Q < K_{eq}$ and at sorption equilibrium ($Q = K_{eq}$), a separate value for net desorption at $Q > K_{eq}$. Differences in ψ result in different relationships between net sorption rates and Q/K_{eq} (or the driving force of the reaction) for net (ad)sorption and desorption processes (Fig. 5).

In principal, this approach can be applied to any type of kinetic 1-site, 2-site or other multi-reaction sorption model. However, specific fitting parameters for ψ have to be included for each site and in each reaction direction (ψ_{ad} and ψ_{de}). Furthermore, mathematical expressions for Q and K_{eq} have to be modified to reflect the specific sorption isotherms selected. These expressions can be found by setting $d[S]/dt$ equal to zero in the individual isotherm-based rate laws (Table 1). As an example, the mathematical framework for the application of this concept to Freundlich and Langmuir isotherms is provided in the Electronic Annex.

Overall, the ψ term can be seen as a descriptor for potential changes in reaction pathways for net adsorption and desorption processes, and as an indicator for the surface sites/reactions that might be most relevant for these changes. Sites with constant ψ values are characterized by constant reaction pathways, and/or elementary reactions that are too fast to capture any significant pathway changes for the overall surface reactions. On the other hand, sites with changing ψ values are involved in overall surface reactions with different net adsorption and desorption pathways, and relatively slow sorption kinetics.

3.2.3. Incorporation of transition state theory-related concept in multi-reaction model

Modeling results suggest different overall rates and reaction pathways for the kinetically-controlled (ad)sorption/desorption processes on site 2. In contrast to site 2, all ψ-terms for site 1 ($\psi_{1,ad}$, $\psi_{1,de}$) could be fixed at values equal to one without causing any substantial decline in the goodness-of-fit value. This implies that potential changes in sorption rates and reaction pathways are irrelevant for the non-linear, equilibrium site 1.

Site 2 allows for the kinetically-controlled, first-order transfer of sorbed Np(V) from site 1 to site 2 ($S_1 \underset{k_{-2}}{\overset{k_2}{\Longleftrightarrow}} S_2$). Applying the TST-related concept, net Np (ad)sorption is described by

$$\frac{d[S_2]_{ad}}{dt} = k_2[S_1]\left(1 - \left(\frac{Q_2}{K_{2,eq}}\right)^{\psi_{2,ad}=1}\right) \qquad (11)$$

and net desorption by

$$\frac{d[S_2]_{de}}{dt} = k_2[S_1]\left(1 - \left(\frac{Q_2}{K_{2,eq}}\right)^{\psi_{2,de}}\right) \qquad (12)$$

The conditional sorption coefficient on site 2 is defined as $Q_2 = [S_2]/[S_1]$, the sorption equilibrium constant as $K_{2,eq} = k_2/k_{-2}$. During fitting, values of Q_2 were calculated from Np(V) solution and surface concentrations at individual time-points in the experiment; values of $K_{2,eq}$ are based on the fitted values of rate constants.

The fitted values of $\psi_{2,ad}$ (=1) and $\psi_{2,de}$ (≈ 0.01) determine the mathematical relationships between the net sorption rates and $Q_2/K_{2,eq}$ (Fig. 5). For all ψ parameters with values of unity ($\psi_{1,ad}$, $\psi_{1,de}$, $\psi_{2,de}$) the model simulates a linear relationship between net (ad)sorption/desorption rates and Q/K_{eq} ratios (Fig. 5). Due to the low value of $\psi_{2,de}$, Np desorption behavior is mainly controlled by the surface-concentration dependent desorption rates on site 2. With $\psi_{2,de} \approx 0.01$, this parameter should be regarded as an empirical fitting parameter. A Temkin coefficient of approximately 100 seems unusual, since typical values range between one and three for dissolution/precipitation kinetics (Oelkers, 2001; Dixit and Carroll, 2007; Yang and Steefel, 2008). In this modeling approach, net sorption rates are dependent on the direction of the surface reaction (individually fitted ψ values), as well as on the actual driving force for the reaction (ΔG). The latter is related to the ratio of Q/K_{eq} (Eqs. (7)–(9)), and a function of Np(V)

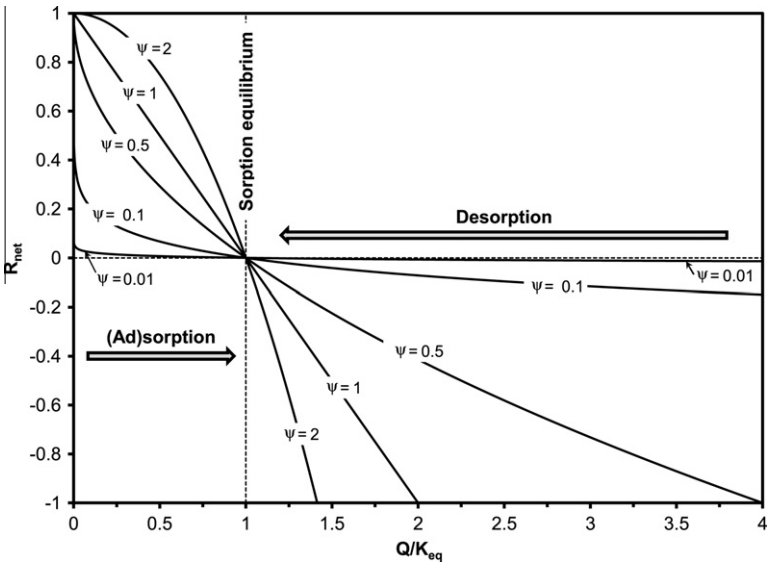

Fig. 5. Relationship between net sorption rates and the ratio Q/K_{eq} (sorption coefficient over equilibrium constant) for different values of ψ plotted over the range of Q/K_{eq} values observed during modeling (see Fig. 6). For simplification, a constant forward rate of $R_+ = 1$ was assumed in Eq. (9). Net (ad)sorption ($R_{net} > 0$) occurs for $Q/K_{eq} < 1$ (top left corner), net desorption ($R_{net} < 0$) for $Q/K_{eq} > 1$ (bottom right corner). ψ -values affect changes in net sorption rates over the course of (ad)sorption and desorption processes.

solution and surface concentrations, which vary over the experimental time-frame. Hence, a plot of the Q/K_{eq} ratios for individual sites allows us to evaluate if sorption equilibria are reached ($Q/K_{eq} = 1$), and how net (ad)sorption/desorption rates change with Q/K_{eq} over the course of the experiment (Fig. 6a). Net (ad)sorption occurs for Q/K_{eq} ratios smaller than one ('undersaturation' of the surface with respect to Np(V)), desorption for ratios greater than one ('oversaturation' with sorbed Np(V)).

Results show a ratio for site 1 ($Q_1/K_{eq,1}$) close to unity over the whole course of the experiment (Fig. 6), which confirms that site 1 represents an 'equilibrium' site. Consequently, the overall sorption kinetics of Np are strongly affected by changes in the driving force for the surface reaction on site 2. For instance, for the (ad)sorption part of the experiment, $Q_2/K_{eq,2}$ ratios substantially increase during both stop-flow events, coming closer to sorption equilibrium conditions at a ratio of 1. During desorption, $Q_2/K_{eq,2}$ ratios decrease after stop-flow events but never completely reach values of one (Fig. 6a). Therefore, site 2 desorption equilibria have not been reached under continuous flow conditions or during stop-flow events. Due to the change in ψ -values for Np (ad)sorption and desorption, net rates on site 2 substantially drop for the desorption part of the experiment (Fig. 6). Furthermore, with decreasing Np surface loads resulting in smaller $Q_2/K_{eq,2}$ ratios over time, absolute values of Np desorption rates decrease over the course of the desorption experiment (Figs. 5 and 6b).

In the context of this 2-site kinetic model, it is interesting to compare maximum neptunium surface concentrations on sites 1 and 2 with the distribution of high and low affinity surface sites. In this experiment, the highest, total neptunium surface concentration was simulated as 3.98×10^{-6} (mol Np g^{-1}), with 3.33×10^{-6} (mol Np g^{-1}) on site 1 (equilibrium site) and 6.47×10^{-7} (mol Np g^{-1}) on site 2 (kinetic site). Hence, at the highest neptunium surface loading, 83.7% and 16.3% of Np(V) was sorbed to equilibrium and kinetic sites, respectively. For comparison, we computed the distribution of low and high affinity surface sites based on an average goethite surface area of 14.2 (m^2 g^{-1}), a total surface site density of 2.3 (sites nm^{-2}), and a fraction of 1% of high affinity surface sites (Dzombak and Morel, 1990). This results in 5.35×10^{-5} (mol sites g^{-1}) low affinity and 5.41×10^{-7} (mol sites g^{-1}) high affinity surface sites. Therefore, our specific modeling results suggest that kinetically-limited sites represent a minimum of 1.2% of total sites, which is in the same concentration range as high affinity surface sites. However, kinetically-limited sites and high affinity surface sites may not necessarily be identical, and further research is needed to investigate specific surface site characteristics.

3.2.4. Relevance of aging processes

The necessity to include consecutive surface sites in kinetic sorption models has previously been interpreted as an indication for aging processes (Ciffroy et al., 2001; Ciffroy et al., 2003; Garnier et al., 2006). Hence, we will compare fitting results for a kinetic 1-site Freundlich model (Fig. 2a) and the multi-reaction Freundlich model described above (Fig. 2b), without including any ψ-terms for simplification.

Both models provide fairly good fits of Np(V) sorption and desorption behavior under continuous flow conditions, but do not capture all system responses to stop-flow events (Fig. 7). A plot of simulated Np surface concentrations on sites 1 and 2 illustrates the importance of slow (site 2) and fast (site 1) sorption reactions in the multi-reaction model (Fig. 8). A good model fit for stop-flow events is largely

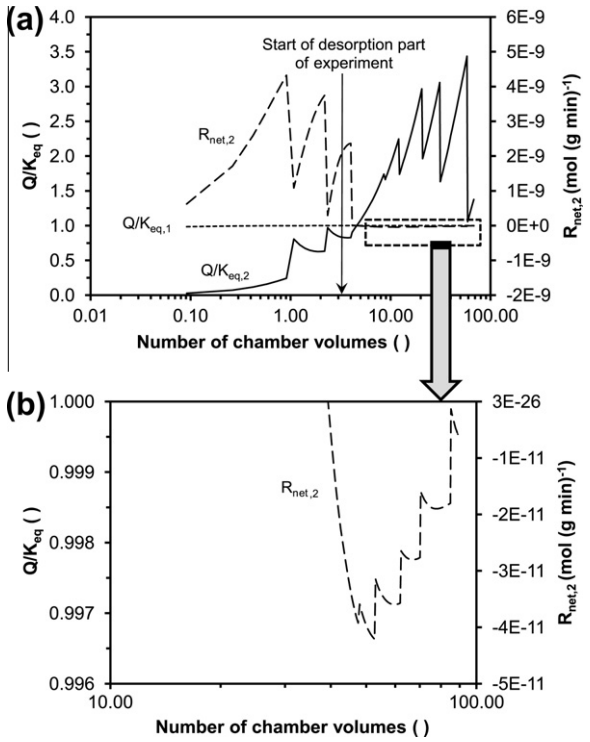

Fig. 6. Ratios of Q/K_{eq} for surface sites 1 and 2 over the course of the Np(V)–goethite flow-cell experiment. Values of Q_1 and Q_2 were calculated based on simulated values of Np(V) solution and surface concentrations; $K_{eq,1}$ and $K_{eq,2}$ were determined from fitted values of corresponding rate constants. (Ad)sorption occurs for ratios <1, desorption for ratios >1.

dependent on the 'appropriate' transfer of Np(V) between these two 'sites'. For example, net Np desorption is only calculated for events, where a decrease in metal concentration on site 2 leads to a concentration increase on site 1. The same behavior is also observed for the TST-related model including a $\psi_{2,de}$-term (Fig. EA-4; Electronic Annex). Hence, the incorporation of two sites with different sorption kinetics allows for different degrees of rate-limitations during short (continuous flow) and long (stop-flow events) sorption equilibration. Overall, these results illustrate the relevance of aging for the successful simulation of Np desorption from goethite over extended time-frames.

In general, neptunium interactions with site 2 could represent a variety of possible secondary surface processes over time, such as the re-distribution of the sorbate over sites with various sorption affinities, or changes in binding strengths of surface complexes, e.g., due to structural changes, or surface-mediated redox transformations (Theis et al., 1988; Smith et al., 2009; Wendling et al., 2009). Furthermore, metal diffusion into goethite pores cannot be ruled out, as this has been shown to be a relevant process for other metal contaminants (Mustafa et al., 2006; Fischer et al., 2007). Previous studies focusing on Np(V) sorption onto Fe-oxide minerals suggest that the following surface chemical processes may be relevant: (1) the transformation of neptunium outer- into inner-sphere complexes, as indicated by X-ray absorption spectroscopy (Jerden and Kropf, 2007), and (2) the surface-mediated reduction of Np(V) to Np(IV), which has been reported for goethite (Jerden and Kropf, 2007) and magnetite (Nakata et al., 2002; Nakata et al., 2004). Furthermore, the decomplexation of ternary metal–carbonato surface complexes over time and surface hydration/dehydration phenomena may also play a role. In any case, chemical system conditions, such as Eh (Nakata et al., 2002; Nakata et al., 2004) and salt composition (Jerden and Kropf, 2007), may largely affect the type of surface complexes formed initially, as well as their later, time-dependent transformations. Clearly, additional experimental studies are needed in order to evaluate the relevance of various physico-chemical processes for Np(V) sorption/desorption behavior in these systems. However, a detailed investigation of Np(V) aging processes on goethite goes beyond the scope of this study.

3.2.5. Evaluation of hysteresis effects and short-term irreversible sorption behavior

Experimental data suggest that hysteresis effects are probably minimal (Fig. 1). Furthermore, the best model fit was achieved without the need to incorporate any specific hysteresis terms. Nevertheless, we decided to further test these results using the following, two model-based approaches.

First, flow-cell data were split into (ad)sorption and desorption branches, and both parts fit with two independent sets of fitting parameters using a multi-reaction Freundlich model without ψ-terms (Fig. 2b). (The Freundlich exponent n_1 was treated as a 'global' fitting parameter in the process.) Fitted rate constants were then used to calculate overall K_d values for Np(V) (ad)sorption/desorption processes taking into account Np(V) reactions on individual sites. (Note that a direct calculation of (ad)sorption/desorption K_d values based on experimental flow-cell data is not possible, as steady-state has clearly not been reached under flow-conditions in the desorption part of the experiment.)

$$K_d = \frac{[S_{Tot}]}{[C]} = \frac{[S_1] + [S_2]}{[C]} \tag{13}$$

At equilibrium conditions, sorbed metal concentrations on sites 1 and 2 can be determined from Eq. (3) and by setting $d[S_2]/dt$ equal to zero in Eq. (4).

$$[S_2] = \frac{k_2}{k_{-2}}[S_1] = \frac{k_2}{k_{-2}} K_F [C]^{n_1} \tag{14}$$

After combining Eqs. (3), (12), and (13), the total surface concentrations and equilibrium K_d values can be computed as

$$[S_{Tot}] = [C]^{n_1} K_F \left(1 + \frac{k_2}{k_{-2}}\right) \tag{15}$$

and

$$K_d = [C]^{(n_1-1)} K_F \left(1 + \frac{k_2}{k_{-2}}\right) \tag{16}$$

The 'split' model accurately simulates system responses to stop-flow events over the whole course of the experiment (Fig. EA-5), and provides an improved goodness-of-fit

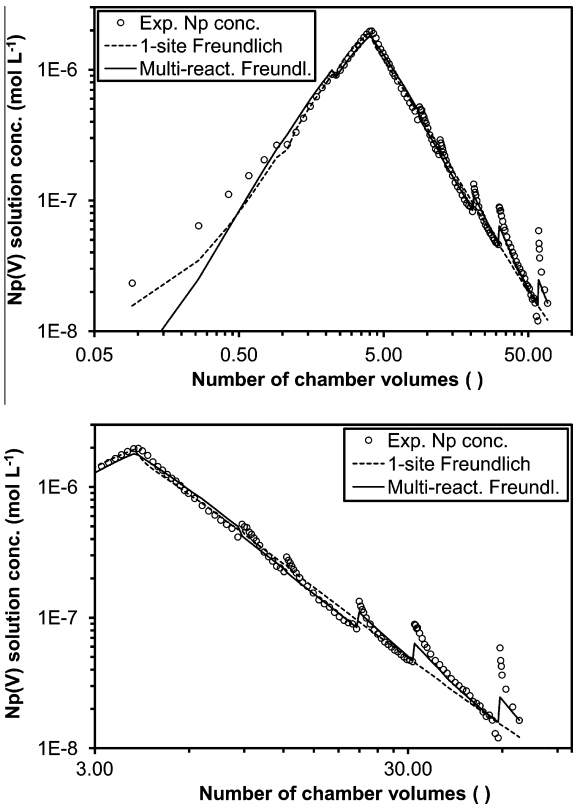

Fig. 7. Comparison of (global) 1-site and multi-reaction Freundlich models (without ψ-terms) suggesting a relevance of aging processes for Np(V) sorption/desorption kinetics on goethite (see text for details).

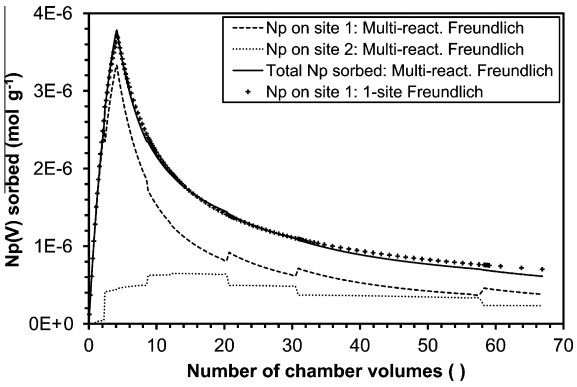

Fig. 8. Neptunium concentrations on various surface sites over the course of the flow-cell experiment as simulated in 1-site and multi-reaction (global) Freundlich models not including any ψ-terms. (For the 1-site model, Np(V) surface concentrations on site 1 are equivalent to total metal concentrations sorbed.).

value relative to a comparable 'global' model (Table 2). Overall K_d values were calculated as 1.50 ± 0.31 and 0.86 ± 0.10 ($L\,g^{-1}$; 95% confidence interval) for the (ad)sorption and desorption parts of the experiment, respectively after arbitrarily assuming a Np(V) solution concentration of 3.16×10^{-6} M. Due to the similarity of these values, sorption hysteresis appears to be very limited.

In the second approach, 'global' and 'split' multi-reaction Freundlich models were extended to include an additional irreversible surface site 3 (Fig. 2d). Despite the increase in the number of fitting parameter(s), model fits are not improved relative to comparable 2-site models, and rate constants for Np transfer from site 2 to site 3 are negligible (Figs. EA-6 and EA-7, Electronic Annex). Overall, within the time-frame (desorption over 32 days) and chemical solution conditions evaluated in the flow-cell experiment, aging processes do not appear to lead to (short-term) irreversible sorption behavior. Nevertheless, irreversible sorption may become relevant at very low metal surface concentrations, below the lowest neptunium surface loading tested in this study (much less than 1%).

3.2.6. Equilibrium versus irreversible sorption behavior

In the following, we combine our results from the model development and the evaluation of specific (kinetic) sorption characteristics. The best model fit was achieved with a multi-reaction Freundlich model including a TST-related ψ-parameter, which suggests that different, molecular-scale pathways may be relevant for Np net (ad)sorption and desorption processes. Hence, rate changes for overall (ad)sorption and desorption reactions may be due to the involvement of a series of different Np surface species depending on the net direction of the surface reaction. For example, metal surface speciation may be changing due to aging processes over time. The relevance of aging in this system was supported by the need to include multiple surface sites in the kinetic model. However, an additional confirmation of this result with experimental data would be useful, e.g. based on results from time-dependent spectroscopic studies or by using a variety of metal isotopes over time. In contrast, hysteresis effects and irreversible sorption behavior were shown to be negligible for the experimental conditions and time-frames evaluated.

Overall, differences in reaction rates appear to be more relevant for the observed 'asymmetry' between (ad)sorption and desorption processes than changes in Np sorption equilibria in terms of hysteresis or irreversible sorption behavior. Sorption rates may primarily change due to differences in overall reaction pathways, while the system still approaches the same sorption equilibrium from both reaction directions (equilibrium sorption). In other words, variations in sorption/desorption rates are not necessarily equivalent to irreversible sorption behavior in this system. The proposed modeling approach based on a TST-related kinetic concept specifically allows for this possibility.

3.2.7. Similarity of best-model concept with similar multi-reaction models

As discussed in detail elsewhere (Barros and Abril, 2005), various configurations of multi-reaction models can lead to mathematically equivalent models, e.g. for parallel and consecutive sorption sites, which complicates the selection of a 'best model fit'. Besides the Freundlich multi-reaction model, similar modeling results and kinetic trends were observed with various, other multi-reaction concepts consisting of two surface sites, set up either in parallel or in series (Fig. 2b and c). The models described in Fig. 2 are generally,

mathematically distinct from each other, but can become comparable under specific conditions, assuming site 1 represents an equilibrium site in all models. For example, a consecutive Freundlich model (Fig. 2b) is a simplification of a 2-parallel-site Freundlich model (Fig. 2c) if the Freundlich exponents for sites 1 and 2 in the parallel model are the same. Second, the kinetic behavior in a consecutive Freundlich and parallel Langmuir model will be similar if both systems depict similar equilibrium sorption behavior on site 1 (same 'curvature' of isotherm), and the Langmuir model shows no surface site limitations.

4. SUMMARY AND CONCLUSIONS

The (ad)sorption and desorption behavior of Np(V) on goethite was investigated using an experimental flow-cell design. This dynamic system allows for the characterization of sorption kinetics at various solution and surface concentrations as well as during continuous flow and stop-flow events. Hence, flow-cell designs allow for a more detailed characterization of hysteresis effects and irreversible sorption behavior than batch systems. Based on our experimental results, Np(V) (ad)sorption to goethite is fairly fast, reaching steady-state conditions within hours. In comparison, metal desorption rates are much slower and appear to continuously decrease over the course of the flow-cell experiment (32.46 days).

Various kinetic models were developed in order to evaluate the relevance of a number of (kinetic) sorption characteristics including aging, hysteresis, and equilibrium versus irreversible sorption behavior. The best model fit was achieved with a 'global' multi-reaction model including (1) an equilibrium Freundlich site (site 1), (2) a kinetically-controlled, consecutive, first-order site (site 2), and (3) a parameter $\psi_{2,de}$, which characterizes desorption rates on site 2 based on a concept related to transition state theory (TST). The fact that simulated adsorption and desorption values of ψ ($\psi_{2,ad} = 1$ and $\psi_{2,de} \approx 0.01$) are different, indicates a difference in overall reaction pathways for Np(V) adsorption and desorption processes. Hence, this approach allows us to link differences in adsorption and desorption kinetics to changes in overall reaction pathways without assuming different adsorption and desorption affinities (hysteresis) or irreversible sorption behavior a priori. In other words, for this system we were able to simulate differences in adsorption and desorption kinetics by assuming variations in reaction pathways, while adsorption and desorption equilibria remained the same.

According to our knowledge, this is the first example of an application of a TST-related kinetic concept to the simulation of contaminant sorption/desorption kinetics on mineral surfaces. The use of the parameter ψ as an indicator for changing overall reaction pathways for net adsorption/desorption processes should be applicable to many other systems besides Np and goethite. However, modeling results and their implications for the relevance of aging, hysteresis and irreversible sorption behavior may strongly depend on the metals and mineral phases under investigation. For instance, different elements may form various types of surface complexes (Garnier et al., 2006), or may be characterized by different pore diffusion rates depending on their ionic radius (Fischer et al., 2007).

Overall, our modeling results suggest the following kinetic characteristics for Np(V) sorption/desorption behavior on goethite:

1. Desorption kinetics are the most important factor controlling Np(V) partitioning between aqueous and solid phases under constant chemical conditions. Desorption rates are substantially slower than (ad)sorption kinetics and show a non-linear dependence on the driving force of the reaction.
2. Aging processes take place after the initial sorption of Np(V) to the mineral surface.
3. Within the range of equilibration time-frames and chemical conditions tested, hysteresis and irreversible sorption behavior play only minor roles, if any. Nevertheless, irreversible sorption may become relevant at low metal surface loadings (much less than 1%), which were not examined in this study.
4. Differences in reaction rates appear to be more relevant for the observed 'asymmetry' between (ad)sorption and desorption processes than changes in Np sorption equilibria in terms of hysteresis or irreversible sorption behavior. Sorption rates may change due to different microscopic reaction pathways, while the system still approaches the same sorption equilibrium from both directions.

In summary, Np desorption reactions are very slow, but they are not irreversible in a thermodynamic sense within the experimental conditions evaluated in this study.

These results have important implications for the mobility of Np(V) in saturated porous media. Under field conditions, the reversibility of Np(V) sorption reactions will limit the relevance of colloid-facilitated transport, as, after its desorption from colloidal surfaces, neptunium will become re-distributed between the groundwater solution and bulk mineral phases. Our data do not justify an assumption of irreversible Np(V) sorption to goethite in transport models, which will exaggerate colloid-facilitated metal mobility. However, for bulk mineral phases slow contaminant desorption rates may potentially create 'continuous source terms', where low contaminant concentrations are continuously desorbed over extended time-frames. The latter may further result in longer tailings of contaminant plumes and extensive time-frames required for site remediation.

ACKNOWLEDGEMENTS

The authors thank S. Carroll and A. F. B. Tompson (Lawrence Livermore National Laboratory, USA) as well as M. Geier (Sandia National Laboratory, USA) for many helpful discussions. This work performed under the auspices of the U.S. Department of Energy by Lawrence Livermore National Laboratory under Contract DE-AC52-07NA27344.

APPENDIX A. SUPPLEMENTARY DATA

Supplementary data associated with this article can be found, in the online version, at doi:10.1016/j.gca.2011.08.014.

REFERENCES

Adamson A. W. (1990) *Physical Chemistry of Surfaces*. John Wiley & Sons, Inc., New York.

Alekseyev V. A., Medvedeva L. S., Prisyagina N. I., Meshalkin S. S. and Balabin A. I. (1997) Change in the dissolution rates of alkali feldspars as a result of secondary mineral precipitation and approach to equilibrium. *Geochim. Cosmochim. Acta* **61**, 1125–1142.

Bar-Tal A., Sparks D. L., Pesek J. D. and Feigenbaum S. (1990) Analyses of adsorption-kinetics using a stirred-flow chamber.1. Theory and critical tests. *Soil Sci. Soc. Am. J.* **54**, 1273–1278.

Barros H. and Abril J. M. (2005) Constraints in the construction and/or selection of kinetic box models for the uptake of radionuclides and heavy metals by suspended particulate matter. *Ecol. Model.* **185**, 371–385.

Braithwaite A., Richardson S., Moyes L. N., Livens F. R., Bunker D. J., Hughes C. R., Smith J. T. and Hilton J. (2000) Sorption kinetics of uranium-238 and neptunium-237 on a glacial sediment. *Czech J. Phys.* **50**, 265–269.

Brantley S. L. (2008) Kinetics of mineral dissolution. In *Kinetics of Water–Rock Interaction* (eds. S. L. Brantley, J. D. Kubicki and A. F. White). Springer, New York.

Buchter B., Hinz C., Gfeller M. and Fluhler H. (1996) Cadmium transport in an unsaturated stony subsoil monolith. *Soil Sci. Soc. Am. J.* **60**, 716–721.

Carroll S., Mroczek E., Alai M. and Ebert M. (1998) Amorphous silica precipitation (60 to 120 degrees C): comparison of laboratory and field rates. *Geochim. Cosmochim. Acta* **62**, 1379–1396.

Celis R. and Koskinen W. C. (1999) An isotopic exchange method for the characterization of the irreversibility of pesticide sorption-desorption in soil. *J. Agric. Food Chem.* **47**, 782–790.

Chairat C., Schott J., Oelkers E. H., Lartigue J. E. and Harouiya N. (2007) Kinetics and mechanism of natural fluorapatite dissolution at 25 degrees C and pH from 3 to 12. *Geochim. Cosmochim. Acta* **71**, 5901–5912.

Choppin G. R. (2006) Actinide speciation in aquatic systems. *Mar. Chem.* **99**, 83–92.

Ciffroy P., Garnier J. M. and Benyahya L. (2003) Kinetic partitioning of Co, Mn, Cs, Fe, Ag, Zn and Cd in fresh waters (Loire) mixed with brackish waters (Loire estuary): experimental and modelling approaches. *Mar. Pollut. Bull.* **46**, 626–641.

Ciffroy P., Garnier J. M. and Pham M. K. (2001) Kinetics of the adsorption and desorption of radionuclides of Co, Mn, Cs, Fe, Ag and Cd in freshwater systems: experimental and modelling approaches. *J. Environ. Radioactiv.* **55**, 71–91.

Comans R. N. J., Haller M. and Depreter P. (1991) Sorption of Cesium on Illite – Nonequilibrium Behavior and Reversibility. *Geochim. Cosmochim. Acta* **55**, 433–440.

Cvetkovic V. (2000) Colloid-facilitated tracer transport by steady random ground-water flow. *Phys. Fluids* **12**, 2279–2294.

Cvetkovic V., Painter S., Turner D., Pickett D. and Bertetti P. 2004 Parameter and model sensitivities for colloid-facilitated radionuclide transport on the field scale. *Water Resour. Res.* **40.**

Dixit S. and Carroll S. A. 2007 Effect of solution saturation state and temperature on diopside dissolution. *Geochem. T.* **8.**

Doherty J. (2004) *PEST-Model Independent Parameter Estimation User Manual*. Watermark Numerical Computing, Brisbane, Australia.

Dozol M., Hagemann R., Hoffman D. C., Adloff J. P., Vongunten H. R., Foos J., Kasprzak K. S., Liu Y. F., Zvara I., Ache H. J., Das H. A., Hagemann R. J. C., Herrmann G., Karol P., Maenhaut W., Nakahara H., Sakanoue M., Tetlow J. A., Baro G. B., Fardy J. J., Benes P., Roessler K., Roth E., Burger K., Steinnes E., Kostanski M. J., Peisach M., Liljenzin J. O., Aras N. K., Myasoedov B. F. and Holden N. E. (1993) Radionuclide migration in groundwaters – review of the behavior of actinides – (Technical Report). *Pure Appl. Chem.* **65**, 1081–1102.

Dzombak D. A. and Morel F. M. M. (1990) *Surface Complexation Modeling: Hydrous Ferric Oxide*. John Wiley & Sons, New York.

Farrell J., Grassian D. and Jones M. (1999) Investigation of mechanisms contributing to slow desorption of hydrophobic organic compounds from mineral solids. *Environ. Sci. Technol.* **33**, 1237–1243.

Fischer L., Brummer G. W. and Barrow N. J. (2007) Observations and modelling of the reactions of 10 metals with goethite: adsorption and diffusion processes. *Eur. J. Soil Sci.* **58**, 1304–1315.

Gao Y., Kan A. T. and Tomson M. B. (2003) Critical evaluation of desorption phenomena of heavy metals from natural sediments. *Environ. Sci. Technol.* **37**, 5566–5573.

Garnier J. M., Ciffroy P. and Benyahya L. (2006) Implications of short and long term (30 days) sorption on the desorption kinetic of trace metals (Cd, Zn, Co, Mn, Fe, Ag, Cs) associated with river suspended matter. *Sci. Total Environ.* **366**, 350–360.

Huang W. L. and Weber W. J. (1997) A distributed reactivity model for sorption by soils and sediments.10. Relationships between desorption, hysteresis, and the chemical characteristics of organic domains. *Environ. Sci. Technol.* **31**, 2562–2569.

Huang W. L., Yu H. and Weber W. J. (1998) Hysteresis in the sorption and desorption of hydrophobic organic contaminants by soils and sediments – 1. A comparative analysis of experimental protocols. *J. Contam. Hydrol.* **31**, 129–148.

Jannasch H. W., Honeyman B. D., Balistrieri L. S. and Murray J. W. (1988) Kinetics of trace-element uptake by marine particles. *Geochim. Cosmochim. Acta* **52**, 567–577.

Jerden, J. L. and Kropf, A. J., 2007. Surface complexation of neptunium(V) with goethite. In: Dunn, D., Poinssot, C., and Begg, B. (Eds.), *Scientific Basis for Nuclear Waste Management XXX*.

Kalmykov S. N., Kriventsov V. V., Teterin Y. A. and Novikov A. P. (2007) Plutonium and neptunium speciation bound to hydrous ferric oxide colloids. *C. R. Chim.* **10**, 1060–1066.

Kaszuba J. P. and Runde W. H. (1999) The aqueous geochemistry of neptunium: dynamic control of soluble concentrations with applications to nuclear waste disposal. *Environ. Sci. Technol.* **33**, 4427–4433.

Keeney-Kennicutt W. L. and Morse J. W. (1984) The interaction of Np(V)2+ with common mineral surfaces in dilute aqueous solutions and seawater. *Mar. Chem.* **15**, 133–150.

Kohler M., Honeyman B. D. and Leckie J. O. (1999) Neptunium(V) sorption on hematite (alpha-Fe_2O_3) in aqueous suspension: The effect of CO_2. *Radiochim. Acta* **85**, 33–48.

Kumata M. and Vandergraaf T. T. (1998) Experimental study on neptunium migration under in situ geochemical conditions. *J. Contam. Hydrol.* **35**, 31–40.

Laird D. A., Yen P. Y., Koskinen W. C., Steinheimer T. R. and Dowdy R. H. (1994) Sorption of atrazine on soil clay components. *Environ. Sci. Technol.* **28**, 1054–1061.

Lasaga A. C. (1998) *Kinetic Theory in the Earth Sciences*. Princeton University Press, Princeton, New Jersey.

Lesan H. M. and Bhandari A. (2003) Atrazine sorption on surface soils: time-dependent phase distribution and apparent desorption hysteresis. *Water Res.* **37**, 1644–1654.

Limousin G., Gaudet J. P., Charlet L., Szenknect S., Barthes V. and Krimissa M. (2007) Sorption isotherms: a review on physical bases, modeling and measurement. *Appl. Geochem.* **22**, 249–275.

Maher K., Steefel C. I., White A. F. and Stonestrom D. A. (2009) The role of reaction affinity and secondary minerals in

regulating chemical weathering rates at the Santa Cruz Soil Chronosequence, California. *Geochim. Cosmochim. Acta* **73**, 2804–2831.

McBride M. B. (1991) Processes of heavy and transition metal sorption by soil minerals. In *Interactions at the Soil Colloid–Soil Solution Interface (NATO Science Series E)* (eds. G. H. Bolt, M. F. Boodt, M. B. McBride and E. B. A. de Strooper). Kluwer Academic Publishers, Dordrecht, The Netherlands.

Millward G. E. and Liu Y. P. (2003) Modelling metal desorption kinetics in estuaries. *Sci. Total Environ.* **314**, 613–623.

Missana T., Garcia-Gutierrez M. and Alonso U. (2004) Kinetics and irreversibility of cesium and uranium sorption onto bentonite colloids in a deep granitic environment. *Appl. Clay Sci.* **26**, 137–150.

Morgan J. J. and Stone A. T. (1985) Kinetics of chemical processes of importance in lacustrine environments. In *Chemical Processes in Lakes* (ed. W. Stumm). John Wiley & Sons, Inc., New York.

Mustafa G., Kookana R. S. and Singh B. (2006) Desorption of cadmium from goethite: effects of pH, temperature and aging. *Chemosphere* **64**, 856–865.

Nagasaki S., Tanaka S. and Suzuki A. (1994) Influence of Fe(III) colloids on Np(V) migration through quartz-packed columns. *J. Nucl. Sci. Technol.* **31**, 143–150.

Nagasaki S., Tanaka S. and Suzuki A. (1999) Sorption of neptunium on bentonite and its migration in geosphere. *Colloid. Surf. A* **155**, 137–143.

Nakata K., Nagasaki S., Tanaka S., Sakamoto Y., Tanaka T. and Ogawa H. (2000) Sorption and desorption kinetics of Np(V) on magnetite and hematite. *Radiochim. Acta* **88**, 453–457.

Nakata K., Nagasaki S., Tanaka S., Sakamoto Y., Tanaka T. and Ogawa H. (2002) Sorption and reduction of neptunium(V) on the surface of iron oxides. *Radiochim. Acta* **90**, 665–669.

Nakata K., Nagasaki S., Tanaka S., Sakamoto Y., Tanaka T. and Ogawa H. (2004) Reduction rate of neptunium(V) in heterogeneous solution with magnetite. *Radiochim. Acta* **92**, 145–149.

Nakayama S. and Sakamoto Y. (1991) Sorption of neptunium on naturally-occurring iron-containing minerals. *Radiochim. Acta* **52–3**, 153–157.

Nyffeler U. P., Li Y. H. and Santschi P. H. (1984) A kinetic approach to describe trace-element distribution between particles and solution in natural aquatic systems. *Geochim. Cosmochim. Acta* **48**, 1513–1522.

Oelkers E. H. (2001) General kinetic description of multioxide silicate mineral and glass dissolution. *Geochim. Cosmochim. Acta* **65**, 3703–3719.

Ogwada R. A. and Sparks D. L. (1986a) A critical-evaluation on the use of kinetics for determining thermodynamics of ion-exchange in soils. *Soil Sci. Soc. Am. J.* **50**, 300–305.

Ogwada R. A. and Sparks D. L. (1986b) Kinetics of ion-exchange on clay-minerals and soil. 2. Elucidation of rate-limiting steps. *Soil Sci. Soc. Am. J.* **50**, 1162.

Saiers J. E. and Hornberger G. M. (1996) The role of colloidal kaolinite in the transport of cesium through laboratory sand columns. *Water Resour. Res.* **32**, 33–41.

Sander M., Lu Y. F. and Pignatello J. J. (2005) A thermodynamically based method to quantify true sorption hysteresis. *J. Environ. Qual.* **34**, 1063–1072.

Schwertmann U. and Cornell R. M. (1991) *Iron Oxides in the Laboratory: Preparation and Characterization*. VCH Verlagsgesellschaft mbH, Weinheim.

Selim H. M. and Amacher M. C. (1997) *Reactivity and Transport of Heavy Metals in Soils*. CRC Press, Inc., Boca Raton.

Selim H. M. and Zhu H. (2005) Atrazine sorption–desorption hysteresis by sugarcane mulch residue. *J. Environ. Qual.* **34**, 325–335.

Seyfried M. S., Sparks D. L., Bartal A. and Feigenbaum S. (1989) Kinetics of calcium magnesium exchange on soil using a stirred-flow reaction chamber. *Soil Sci. Soc. Am. J.* **53**, 406–410.

Shirvani M., Kalbasi M., Shariatmadari H., Nourbakhsh F. and Najafi B. (2006) Sorption–desorption of cadmium in aqueous palygorskite, sepiolite, and calcite suspensions: Isotherm hysteresis. *Chemosphere* **65**, 2178–2184.

Sing K. S. W., Everett D. H., Haul R. A. W., Moscou L., Pierotti R. A., Rouquerol J. and Siemieniewska T. (1985) Reporting physisorption data for gas solid systems with special reference to the determination of surface-area, porosity (recommendations 1984). *Pure Appl. Chem.* **57**, 603–619.

Skopp J. and McCallister D. (1986) Chemical-kinetics from a thin disk flow system – theory. *Soil Sci. Soc. Am. J.* **50**, 617–622.

Smith S. C., Douglas M., Moore D. A., Kukkadapu R. K. and Arey B. W. (2009) Uranium extraction from laboratory-synthesized, uranium-doped hydrous ferric oxides. *Environ. Sci. Technol.* **43**, 2341–2347.

Sparks D. L. (2000) New frontiers in elucidating the kinetics and mechanisms of metal and oxyanion sorption at the soil mineral/water interface. *J. Plant. Nutr. Soil. Sc.* **163**, 563–570.

Steefel C. I. (2008) Geochemical kinetics and transport. In *Kinetics of Water–Rock Interaction* (eds. S. L. Brantley, J. D. Kubicki and A. F. White). Springer, New York.

Stumm W. (1992) *Chemistry of the Solid–Water Interface. Processes at the Mineral–Water and Particle–Water Interface in Natural Systems*. John Wiley & Sons, Inc., New York.

Thakur P., Moore R. C. and Choppin G. R. (2006) Np(V)O-2(+) sorption on hydroxyapatite-effect of calcium and phosphate anions. *Radiochim. Acta* **94**, 645–649.

Theis T. L., Iyer R. and Kaul L. W. (1988) Kinetic studies of cadmium and ferricyanide adsorption on goethite. *Environ. Sci. Technol.* **22**, 1013–1017.

Thompson R. C. (1982) Neptunium – the neglected actinide – a review of the biological and environmental literature. *Radiat. Res.* **90**, 1–32.

Undabeytia T., Nir S., Rytwo G., Serban C., Morillo E. and Maqueda C. (2002) Modeling adsorption–desorption processes of Cu on edge and planar sites of montmorillonite. *Environ. Sci. Technol.* **36**, 2677–2683.

Viswanathan H. S., Robinson B. A., Valocchi A. J. and Triay I. R. (1998) A reactive transport model of neptunium migration from the potential repository at Yucca Mountain. *J. Hydrol.* **209**, 251–280.

Wendling L. A., Ma Y. B., Kirby J. K. and McLaughlin M. J. (2009) A predictive model of the effects of aging on cobalt fate and behavior in soil. *Environ. Sci. Technol.* **43**, 135–141.

Yang L. and Steefel C. I. (2008) Kaolinite dissolution and precipitation kinetics at 22 degrees C and pH 4. *Geochim. Cosmochim. Acta* **72**, 99–116.

Zhu H. X. and Selim H. M. (2000) Hysteretic behavior of metolachlor adsorption–desorption in soils. *Soil Sci.* **165**, 632–645.

Associate editor: Michael L. Machesky